SUPPLEMENTARY INFORMATION

DEFICIENCY OR INHIBITION OF THE OXYGEN SENSOR PHD1 INDUCES HYPOXIA TOLERANCE BY REPROGRAMMING BASAL METABOLISM

Julián Aragonés*, Martin Schneider* Katie Van Geyte*, Peter Fraisl*, Tom Dresselaers, Massimiliano Mazzone, Ruud Dirkx, Serena Zacchigna, Hélène Lemieux, Nam Ho Jeoung, Diether Lambrechts, Tammie Bishop, Peggy Lafuste, Antonio Diez-Juan, Sarah K. Harten, Pieter VanNoten, Katrien De Bock, Carsten Willam, Marc Tjwa, Alexandra Grosfeld, Rachel Navet, Lieve Moons, Christophe Deroose, Bhathiya Wijeyekoon, Johan Nuyts, Peter Vermaelen, Benedicte Jordan, Florea Lupu, Mieke Dewerchin, Chris Pugh, Phil Salmon, Luc Mortelmans, Bernard Gallez, Frans Gorus, Johan Buyse, Francis Sluse, Robert A. Harris, Erich Gnaiger, Peter Hespel, Paul Van Hecke, Frans Schuit, Paul Van Veldhoven, Peter Ratcliffe, Myriam Baes, Patrick Maxwell and Peter Carmeliet

SUPPLEMENTARY NOTES

GENERATION OF MICE LACKING *PHD1*

To inactivate the *Phd1* gene, we constructed targeting vectors in which a fragment encoding part of the catalytic domain conferring the prolyl hydroxylase activity [1], (exon 2 and 3 for *Phd1*), was replaced by a neomycin phosphotransferase selection cassette (Supplementary Figure 1). The targeting vector was electroporated in embryonic stem (ES) cells and homologous recombination was confirmed by appropriate Southern blot analysis (Supplementary Figure 1). Targeted ES cell clones were used to generate *Phd1*$^{-/-}$ mice, which were born at the expected Mendelian frequencies and were healthy.

NORMAL ERYTHROPOIESIS, OXYGEN DELIVERY, VASCULARIZATION AND MYOGLOBIN LEVELS IN *PHD1*$^{-/-}$ MICE

ERYTHROPOIESIS & OXYGEN DELIVERY: *Phd1*$^{-/-}$ mice had normal hematocrits (31.4 ± 0.9% in wild-type mice versus 32.9 ± 1.2% in *Phd1*$^{-/-}$ mice; n = 8; P = n.s), hemoglobin levels (not shown), and arterial blood gases (PaO_2 and O_2 saturation: 132 ± 6 mmHg and 98.5 ± 0.4% in wild-type mice versus 132 ± 7 mmHg and 98.1 ± 0.4% in *Phd1*$^{-/-}$ mice; n = 5; P = n.s.).

Therefore induced erythropoiesis or oxygen delivery does not explain *Phd1*$^{-/-}$ myofibers protection.

VASCULARIZATION: At seven days after hindlimb ischemia, the total number of collateral side branches was not increased in the adductor region in *Phd1*$^{-/-}$ limbs (second-generation collateral side branches/mm^2: 22.7 ± 3.1 in wild-type mice versus 22.5 ± 5 in *Phd1*$^{-/-}$ mice; *n* = 7; *P* = n.s.). The collateral perfusion area, representing the sum of the luminal areas of all secondary and tertiary collaterals, was also not significantly altered in *Phd1*$^{-/-}$ limbs (total collateral perfusion area in μm^2/mm^2: 2,290 ± 282 in wild-type mice versus 2,560 ± 241 in *Phd1*$^{-/-}$ mice; *n* = 7; *P* = n.s.). Moreover, capillary density, assessed in viable crural muscle areas after seven days of ischemia, was unaltered in *Phd1*$^{-/-}$ mice (capillaries/mm^2: 720 ± 80 in wild-type mice versus 702 ± 56 in *Phd1*$^{-/-}$ mice; *n* = 7; *P* = n.s.). In accordance with these findings, mRNA levels of *Vegf* were similar in baseline conditions and comparably increased at 4 to 6 hours after ischemia in both genotypes (not shown), altogether indicating that the hypoxic angiogenic stimulus and revascularization response were comparable in both genotypes.

MYOGLOBIN: Myoglobin, a cytoplasmic hemoprotein expressed in cardiac myocytes and oxidative skeletal muscle fibers, reversibly binds O_2, therefore serving as an intracellular oxygen supply/buffering system. By qRT-PCR analysis, myoglobin transcript levels were unaltered in *Phd1*$^{-/-}$ myofibers (not shown). ELISA revealed also no significant differences in myoglobin protein levels in soleus muscle (μg myoglobin/mg total protein: 40.6 ± 8.8 in wild-type versus 35.5 ± 6.6 in *Phd1*$^{-/-}$; *n* = 3; *P* = n.s.) and gastrocnemius muscle (μg myoglobin/mg total protein: 10.8 ± 1.04 in wild-type versus 9.46 ± 0.28 in *Phd1*$^{-/-}$; *n* = 3; *P* = n.s.). In addition, when analyzing active myoglobin content employing a peroxidase-based activity assay [2], we could not detect any genotypic differences in soleus muscle (μg O_2 bound myoglobin/mg total protein: 69.8 ± 7.6 in wild-type versus 79.7 ± 12.4 in *Phd1*$^{-/-}$; *n* = 5; *P* = n.s.) or gastrocnemius muscle (μg O_2 bound myoglobin/mg total protein: 21.7 ± 2.1 in wild-type versus 25.7 ± 4.1 in *Phd1*$^{-/-}$; *n* = 5; *P* = n.s.).

NORMAL VASODILATION AFTER FEMORAL ARTERY LIGATION IN *PHD1*$^{-/-}$ MICE

Since enhanced reactive vasodilation of pre-existing collateral vessels after femoral artery ligation might also account for muscle survival in *Phd1*$^{-/-}$ limbs and Hif's induce a vasodilatory response, we monitored the perfusion of skin vessels (as surrogate for the unaccessible deeper collateral vessels) by laser-Doppler imaging. Skin perfusion increased significantly during the first six hours of ischemia, however, this compensatory increase was comparable in both genotypes (fold-increase of ischemic / contralateral perfusion ratio after 6 hours of ischemia: 1.9 ± 0.3 in wild-type mice versus 1.5 ± 0.3 in *Phd1*$^{-/-}$ mice; $n = 3$; P = n.s.).

PRESERVED MITOCHONDRIAL PERFORMANCE IN ISCHEMIC *PHD1*$^{-/-}$ MYOFIBERS

To assess whether mitochondrial performance was better preserved in ischemic *Phd1*$^{-/-}$ myofibers because of the reduced oxidative stress, we measured mitochondrial respiration rates of skeletal muscle mitochondria, isolated from mice in baseline conditions and at 6 hours after femoral artery ligation. The activity of the respiratory electron transfer chain was determined by measuring how rapidly mitochondria consumed a fixed amount of oxygen in the absence of ADP (*state 2* respiration) and in the presence of ADP (when oxygen consumption is enhanced to generate ATP; *state 3* respiration). We focused on *state 3* respiration as it is more sensitive to ischemic insults than *state 2* respiration. Succinate was added as an oxidizable substrate and electron donor to complex II of the respiratory chain. Because large amounts of mitochondria were required to perform these measurements, gastrocnemius muscles from 6 mice were pooled; data of one of two representative experiments are shown.

In wild-type mice, ischemia caused a 35% reduction in *state 3* respiration rate (state 3 respiration rate, relative to the state 2 respiration rate in wild-type mice at normoxic conditions: 3.2 in normoxic versus 2.1 in hypoxic muscle). In contrast, in *Phd1*$^{-/-}$ mice, ischemia only insignificantly reduced *state 3* respiration rate by 7% (state 3 respiration rate, relative to the state 2 respiration rate in normoxic wild-type mitochondria: 2.9 in normoxic versus 2.7 in hypoxic muscle), indicating that mitochondrial function was not (or only minimally) impaired in *Phd1*$^{-/-}$ muscle. Thus, in the absence of Phd1, mitochondria are capable of functioning (relatively) normally, even after exposure to severe ischemia.

FATTY ACID OXIDATION IN ISCHEMIC *PHD1*$^{-/-}$ FIBERS

Oxidation of [U-^{13}C]-fatty acids was undetectable in ischemic wild-type myofibers, while proceeding at some residual level in ischemic *Phd1*$^{-/-}$ muscles ([4,5-$^{13}C_2$]-glutamate peak, % of total creatine: undetectable (<0.007%) in wild-type mice versus 0.06 ± 0.02% in *Phd1*$^{-/-}$ muscle; n = 6; P < 0.05). Compared to the corresponding baseline values, fatty acid oxidation in ischemic wild-type and *Phd1*$^{-/-}$ myofibers proceeded at <5% and 50% of its normal rate, respectively.

EVALUATION OF EFFICIENCY AND SPECIFICITY OF *PHD1* SPECIFIC KNOCKDOWN

The efficiency and specificity of *shPhd1*^{KD} and *shPhd1*^{CTR} were first tested in cultured murine C2C12 myoblast cells. Compared to non-transfected cells, transfection of C2C12 cells with *shPhd1*^{CTR} did not affect *Phd1* transcript levels (mRNA copies PHD1/10^3 mRNA copies ß-actin: 12.0 ± 1.0 after vehicle versus 11.3 ± 0.3 after *shPhd1*^{CTR}; n = 4; P = n.s.). In contrast, *shPhd1*^{KD} efficiently lowered *Phd1* mRNA levels by 72 % (mRNA copies *Phd1*/10^3 mRNA copies *ß-actin*: 3.4 ± 0.5 after *shPhd1*^{KD}; n = 4; P < 0.05 versus *shPhd1*^{CTR}). *shPhd1*^{KD} did not knock down *Phd2* or *Phd3* (not shown). We then injected and electroporated these constructs into the muscle fibers *in vivo*, as this method is very efficient and causes negligible muscle damage and inflammation.

The constructs were electroporated five days prior to the ligation of the femoral artery because of two reasons: (i) to achieve sufficient elimination of the pre-existing *Phd1* transcripts prior to the induction of ischemia; and (ii) to avoid death of ischemic myofibers before their *Phd1* transcript levels would be sufficiently reduced to provide protection. Both the right and left hindlimb muscles were electroporated, but only the right femoral artery was ligated, permitting us to use the right legs for histological scoring of muscle necrosis and the left muscles for RNA analysis. To obtain sufficiently low endogenous *Phd1* levels after *Phd1* knockdown, we used *Phd1*$^{+/-}$ mice, which only expressed 50% of the *Phd1* transcript levels present in wild-type mice (not shown).

SUPPLEMENTARY EXPERIMENTAL METHODS

TARGETING VECTORS AND GENE INACTIVATION

For construction of the *Phd1* targeting vector, the following fragments were cloned in pKOScramblerNTKV-1908 (from 5' to 3'): a 5 Kb EcoRV/XhoI fragment located 0.85 Kb upstream of exon 2 (5' homologous flank), a neomycin phosphotransferase (neo) resistance cassette in opposite orientation, a 1 Kb XbaI/EcoRV fragment located 0.15 Kb downstream of exon 3 (3' homologous flank), and a thymidine kinase selection cassette. ES cells (129 SvEv background) were electroporated with the linearized targeting vector for *Phd1* as described [3]. Resistant clones were screened for homologous recombination by Southern blotting (Supplementary Figure 1) and PCR (not shown). Correctly recombined ES cell clones were aggregated with morula stage embryos. To obtain $Phd1^{+/-}$ germline offspring in a 50% Swiss / 50% 129 background, chimeric male mice were intercrossed with wild-type Swiss females. Subsequently, heterozygous breeding pairs were established to generate homozygous $Phd1^{-/-}$ progeny. Housing and all experimental animal procedures were approved by the Institutional Animal Care and Research Advisory Committee of the K.U. Leuven.

KNOCKDOWN OF *PHD1* OR *PPAR* IN MICE AND QUANTITATIVE REAL-TIME PCR

shPhd1^{KD} and *shPpar*^{KD} DNA constructs were designed as described (www.invitrogen.com/rnai) to produce short hairpin interference RNA against *Phd1* or *Ppar* *in vivo*. As controls, we used appropriate *shPhd1*^{CTR} and *shPpar*^{CTR} constructs, which differed from *shPhd1*^{KD} and *shPpar*^{KD} by a mismatch of 10 nucleotides in the sequence of *Phd1* and *Ppar*, respectively.

For sequence information on shRNA oligonucleotides, forward and reverse primers and probes, labeled with fluorescent dye (FAM) and quencher (TAMRA), used for quantitative real-time PCR, please refer to Supplementary Table 1.

MYOFIBER TYPING

Transverse cryostat sections of hindlimb muscles were stained with primary monoclonal antibodies directed against fast myosin type IIA and slow myosin type I (Developmental studies Hybridoma Bank, IA, USA; dilution 1/20), and secondary antibodies

Alexa Fluor 350 anti-mouse IgG1 (Molecular Probes, Leiden, The Netherlands) and FITC-anti-mouse (Southern Biotechnology Associates, Birmingham, AL, USA). Fiber size, capillary density and intercapillary distance were quantified on eight entire muscle sections (each 320 µm apart).

INDIRECT CALORIMETRY

Oxygen consumption was simultaneously determined on ad libitum fed, group-housed animals (group A: *n* = 5 for each genotype, group B: *n* = 7 for each genotype, 12 weeks old, male and female mice) via indirect calorimetry by using an open-circuit calorimeter unit [4]. Prior to the measurements the animals were allowed to acclimatize to the chambers for 2 days; measurements were taken during 3 days (with respecting light and night cycles). All mice were weighed individually at the beginning and the end of the 3 days trial; oxygen consumption and carbon dioxide production measurements were taken at 15 min intervals for 72 hours. The data generated represent the mean oxygen consumption per ml per gram per hour (expressed as O_2 consumption: ml per hour per gram body weight).

MITOCHONDRIAL RESPIRATION IN PERMEABILIZED MYOFIBERS

Mitochondrial respiration was determined using high-resolution respirometry (Oroboros Oxygraph-2k), using the DatLab Software for data acquisition and analyses (Oroboros Instruments, Innsbruck, Austria) [5,6]. In detail, soleus muscle was dissected from animals and put immediately into BIOPS/relaxing solution (Ca^{2+}/EGTA buffer (10 mM), free calcium (0.1 µM), imidazole (20 mM), K^+/4-morpholinoethanesulfonic acid (MES) (50 mM), dithiothreitol (DTT; 0.5 mM), $MgCl_2$ (6.56 mM), ATP (5.77 mM), phosphocreatine (15 mM), taurine (20 mM), pH 7.1). Individual fiber bundles were separated with two pairs of sharp forceps, achieving a high degree of fiber separation. The fiber bundles were permeabilized for 30 min in 2 ml of ice-cold relaxing solution containing saponin (50 µg/ml). After rinsing in respiration medium (MiR05; Oroboros, Innsbruck, Austria) containing sucrose (110 mM), potassium lactobionate (60 mM), EGTA (0.5 mM), $MgCl_2$ (3 mM), taurine (20 mM), KH2PO4 (10 mM), HEPES (20 mM), sucrose (110 mM), BSA (1 g/l), pH 7.1, the muscle bundles were blotted and wet weight was measured on a balance controlled for constant relative humidity, so that

all biopsy samples were hydrated to the same degree. The muscle bundles were then immediately transferred into Oxygraph-2k chambers containing respiration medium at 37°C in the O_2 concentration range of 600 µM declining to 200 µM, thus preventing oxygen limitation of respiration [6]. All measurements of respiration were made in quadruplicate, simultaneously. Resting respiration (state 2, absence of adenylates) was measured after the addition of malate (2 mM) and pyruvate (5 mM) as the complex I substrate supply, and then state 3 respiration was assessed by the addition of ADP (2.5 mM). The integrity of the outer mitochondrial membrane was assessed by the addition of cytochrome c (10 µM); no stimulation of respiration was observed. Subsequent addition of glutamate (10 mM) and succinate (10 mM) provided state 3 respiration with convergent electron input to complexes I and II [7]. The addition of rotenone (0.5 µM) resulted in inhibition of complex I for examination of O_2 flux with complex II substrate alone, while atractyloside (50 mM) was added to inhibit ATP/ADP translocase, which allowed assessing resting respiration in the absence of phosphorylation. In separate experiments, the lack of compensatory activation of respiration by fatty acid oxidation was assessed by the addition of the short chain fatty acid octanoyl carnitine (10 mM) while electron input into complexes I and II was active.

ASSESSMENT OF VASCULARIZATION

For assessment of re-vascularization, bismuth gelatino-angiography was carried out, and arterioles branching directly from pre-existing collaterals, connecting the femoral and saphenous artery in the adductor region of the thigh, were quantified by morphometry as described on histological cross sections after 7 days [8]. Side branches were categorized as second or third generation according to their luminal area (> 300 µm, < 300 µm, respectively). For micro-CT angiography, hindlimbs were perfused with a solution containing 30% barium sulfate and 5% gelatine, dissected in toto, and the crural vasculature was imaged using a high-resolution micro-CT imaging system (SkyScan-1172, Skyscan, Aartselaar, Belgium), with a voltage of 50 kVp and a current of 200 µA. Blood flow in non-operated and ligated limbs was measured applying 15 µm fluorescent microspheres (1×10^6 beads per ml, Molecular Probes, Eugene, Oregon) after maximal vasodilation with sodium nitroprusside (50 ng/ml, Sigma) as described [9,10].

TRANSMISSION ELECTRON MICROSCOPY

Quantification was performed according to Weibel's standard stereologic principles for electron microscopy [11], with the aid of a 84-testline grid superimposed over each EM picture (length of short line segment = 0.25 µm; total length of test line = 21 µm). The volume fraction occupied by mitochondriae (Vmi) was determined as the number of test points lying on trans-sections of mitochondria, divided by the number of total points on the test grid. In order to determine the collective surface area of mitochondrial cristae (Smc), we counted the number of intersections (Ni) between test lines and the surface contour of mitochondrial cristae. Smc was subsequently calculated as Ni per test line length, multiplied by 4. In addition, the cristae surface-to-mitochondrial volume ratio was calculated.

NMR SPECTROSCOPY TO DETERMINE ATP CONTENT AND SUBSTRATE OXIDATION

In vivo ^{31}P NMR spectroscopy experiments on lower limbs were performed at 188 MHz in a Bruker Biospec (Karlsruhe, Germany), equipped with a horizontal 4.7 Tesla superconducting magnet, using a 10 mm diameter solenoid transmit-receive coil. Prior to the measurement, mice were anaesthetized with sodium pentobarbital (50 mg/kg body weight Nembutal, Sanofi, Belgium). The hindlimbs were positioned directly inside the coil, and serial ^{31}P NMR spectra were acquired every 3 min during 2 h (30 degree pulse of 9 µs to reduce saturation effects, total repetition time (TR)=1.4 s, number of averages (NA)=128; no proton decoupling). The peak intensities of PCr, Pi and ATP resonances were quantified with the jMRUI software package. The pH was determined from frequency shift of the P_i versus PCr peak. Saturation factors were measured separately and peak amplitudes were corrected accordingly. For *in vivo* determination of glucose and fatty acid oxidation rates in the hindlimbs ^{13}C-tracer labeled compounds (50 mg of [U-^{13}C]-glucose and [U-^{13}C]-fatty acids, respectively) were injected intravenously during 60 minutes. [U-^{13}C]-fatty acids was delivered bound to 3% BSA. After perfusion, muscle samples were rapidly excised and immediately frozen in liquid nitrogen. Following homogenization in perchloric acid, precipitation of $HClO_4$ and pH adjustment (pH = 7.5 ± 0.5), samples were dried and resuspended in D_2O prior to analysis. [1H]- ^{13}CNMR analysis (pulse angle 45deg, TR = 2.5s, scan time = 18-48h, ^{1}H-decoupled, NOE enhanced) revealed the presence of [4,5-$^{13}C_2$]-glutamate, which is formed

during oxidation of [U-^{13}C]-glucose and [U-^{13}C]-fatty acids in the TCA cycle, thus indicating the extent of [U-^{13}C]-glucose- or [U-^{13}C]-fatty acid oxidation. Resonances of newly formed [3,-$^{13}C_1$]- and [3,4,5-$^{13}C_3$]- glutamate were not reliably detectable, we measured the area under the curve (AUC) of the *de novo* formed [4,5-$^{13}C_2$]-glutamate NMR peaks, which were corrected for the total creatine (creatine and phophocreatine) peaks intensities (similar results were obtained when normalizing to taurine). Peak intensities of lactate, succinate, glutamate and total creatine were quantified by integration after baseline correction, using the spectrometer processing software.

DETERMINATION OF GLYCOGEN

Muscle glycogen was measured based on the hexokinase method after acid hydrolysis [12].

ASSESSMENT OF MUCSLE NECROSIS

Microscopic analysis of crural muscle section was performed with a Zeiss Axioplan 2 imaging microscope, equipped with an Axiocam HrC camera and KS300 morphometry software (Zeiss). The cross-sectional areas of viable and necrotic zones were quantified on eight entire sections (each 320 µm apart) of the crural muscles. Necrotic muscle area was expressed in absolute mm^2, as no significant genotypic differences were observed in the total muscle area. For all experiments, except the electroporation studies, the necrotic muscle area was measured in all crural muscles (gastrocnemius, plantaris and soleus). For the PHD knockdown, the necrotic muscle area was measured in the plantaris muscle, as this muscle expressed most of the shRNA constructs (as evidenced after electroporation of a GFP expressing construct) without exhibiting any signs of cellular damage due to the electroporation alone.

MYOGLOBIN DETERMINATION

Skeletal muscle myoglobin content was determined using a sensitive ELISA for murine myoglobin. Therefore samples were prepared using the NE-PER Nuclear and Cytoplasmic Extraction Kit (Pierce Biotechnology Inc., Rockford, IL) and the ELISA was carried out

according to the manufacturers instructions (Life Diagnostics Inc., West Chester, PA). In addition, concentrations of active myoglobin in murine muscle samples were assessed by a peroxidase-based activity assay as previously described [2]. In brief, samples were homogenized in a solution (0.25–0.5 ml/mg dry weight) containing 80 mM KCl and 50 mM Tris-HCl, pH 8.0, on ice for 1.5–2 min. The homogenate was centrifuged at 5000 x g for 10 min at 4°C and 200 µl supernatant was added to the reaction medium. The reaction medium consisted of 760 µl water, 40 µl ethanol containing 50 mM ortho-tolidine (Sigma; St Louis, MO), and 200 µl of 1 M tertiary-butyl-hydroperoxide (Sigma). After 60 min of incubation at room temperature (22–25°C) the absorbance was determined at 436 nm. Equine myoglobin (>99% purity; Sigma), dissolved in the homogenization buffer, was used as a standard.

MEASUREMENT OF GLUTATHIONE

Gastrocnemius samples were homogenized in 5% metaphosphorous buffer containing 1mM DETPA. Tissues were glass-to-glass homogenized at 0°C, centrifuged (10 min; 4°C) and the supernatant used to measure total and oxidized glutathione. 100 µl of buffer was used per 10 mg of tissue. For total glutathione, 10 µl of supernatant as well as blank and standard curves (0.25-10 nmoles) were incubated with 5,5'-dithiobis-(2-nitrobenzoic acid) (DTNB). DNTB reacts with G-SH to generate GS-SG and 5-thio-2-nitrobenzoic acid (TNB; peak absorbance at 420 nm); the GS-SG formed as well as oxidized present in the samples are back-reduced to GSH by glutathione reductase coupled to NADPH oxidation. In this cycling assay, concentrations of the reactants are chosen so that the rate of color formation is linear with time, with the slope of the line (absorbance/time (min); A/t (min)) being directly proportional to the concentration of total glutathione (GSH + GS-SG; GSt). Assay mixtures contained: 10 µl of supernatant, 1100 µl of phosphate buffer (KH_2P0_4, pH7 + 1 mM EDTA), 20 µl DNTB, 50 µl daily-prepared NADPH (1 mg/ml), and 1 unit of glutathione reductase. Oxidized glutathione was measured similarly except that reduced glutathione was masked by incubation with N-ethyl maleimide (NEM). Assay mixtures contained: 100 µl of supernatant, 50 µl of metaphosphorous buffer, 300 µl NEM, 20 mM and 100 µl of 1:1 solution KOH/MOPS buffer (pH 7). NEM-derivatized reduced glutathione was excluded by exposure of whole samples to C18 cartridges (Bond Elut C18, 500mg; Varian Benelux, Sint-Katelijne-Waver, Belgium). Oxidized glutathione was eluted from the column in 1950 µl and the 100 µl was

assayed as above using DNTB derivation.

PDC ACTIVITY DETERMINATION, MITOCHONDRIAL ENZYMATIC ASSAYS AND MUSCLE METABOLITES

Assays for determination of Pyruvate Dehydrogenase Complex (PDC), aconitase, citrate synthasea and succinate dehydrogenase activity were performed as described [13,14]. Metabolites were measured in $HClO_4$ extracts of liver by enzymatic methods [15].

MITOCHONDRIAL RESPIRATION MEASUREMENTS IN ISCHEMIC LIMBS

Mitochondria were isolated from ischemic limbs 6 hours after vascular ligation. For each experiment, crural muscles from 6 limbs were pooled in order to obtain a sufficient sample size. After fat and connective tissue removal, muscles were minced and homogenized in an ice-cold medium containing 100 mM sucrose, 100 mM KCl, 1 mM K_2HPO_4, 0.1 mM EGTA, 0.2% BSA, and 50 mM Tris-Hcl, pH7.4 as previously described [16,17]. Respiration of skeletal muscle mitochondria was measured using a Clark type electrode with 10 mM succinate (plus 5 µM rotenone) as an oxidizable substrate in 1.2 ml of an air saturated incubation medium. *State 3* respiration was measured by an ADP pulse method after ADP was added in limiting amounts (180 µM).

FENOFIBRATE TREATMENT

To assess the muscle protective effect of the PPAR agonist fenofibrate, wild-type mice received fenofibrate (15mg/day; Cayman Chemical, Ann Arbor, MI, USA) by gavage, or vehicle alone for ten days prior to femoral artery ligation. Tissue necrosis was subsequently analyzed on histological sections of the crural muscles as outline above; and mRNA expression of putative Ppar target genes analyzed by quantitative RT-PCR in muscles from healthy limbs. In accordance with previous reports [18,19], the fenofibrate dosage used for this experiment did not induce toxic side effects, or weight reduction.

REFERENCES

1. Epstein, A.C. et al. C. elegans EGL-9 and mammalian homologs define a family of dioxygenases that regulate HIF by prolyl hydroxylation. *Cell* **107**, 43-54 (2001).

2. Lee-de Groot, M.B., Tombe, A.L. & van der Laarse, W.J. Calibrated histochemistry of myoglobin concentration in cardiomyocytes. *J Histochem Cytochem* **46**, 1077-84 (1998).
3. Stalmans, I. et al. Arteriolar and venular patterning in retinas of mice selectively expressing VEGF isoforms. *J Clin Invest* **109**, 327-36 (2002).
4. Buyse, J. et al. Energy and protein metabolism between 3 and 6 weeks of age of male broiler chickens selected for growth rate or for improved food efficiency. *Br Poult Sci* **39**, 264-72 (1998).
5. Kuznetsov, A.V. et al. Mitochondrial defects and heterogeneous cytochrome c release after cardiac cold ischemia and reperfusion. *Am J Physiol Heart Circ Physiol* **286**, H1633-41 (2004).
6. Gnaiger, E. Oxygen conformance of cellular respiration. A perspective of mitochondrial physiology. *Adv Exp Med Biol* **543**, 39-55 (2003).
7. Boushel, R. et al. Patients with type 2 diabetes have normal mitochondrial function in skeletal muscle. *Diabetologia* **50**, 790-6 (2007).
8. Carmeliet, P. et al. Synergism between vascular endothelial growth factor and placental growth factor contributes to angiogenesis and plasma extravasation in pathological conditions. *Nat Med* **7**, 575-83 (2001).
9. Kobayashi, N., Kobayashi, K., Kouno, K., Horinaka, S. & Yagi, S. Effects of intra-atrial injection of colored microspheres on systemic hemodynamics and regional blood flow in rats. *Am J Physiol* **266**, H1910-7 (1994).
10. Luttun, A. et al. Revascularization of ischemic tissues by PlGF treatment, and inhibition of tumor angiogenesis, arthritis and atherosclerosis by anti-Flt1. *Nat Med* **8**, 831-40 (2002).
11. Weibel, E.R., Kistler, G.S. & Scherle, W.F. Practical stereological methods for morphometric cytology. *J Cell Biol* **30**, 23-38 (1966).
12. Jansson, E., Hjemdahl, P. & Kaijser, L. Epinephrine-induced changes in muscle carbohydrate metabolism during exercise in male subjects. *J Appl Physiol* **60**, 1466-70 (1986).
13. Hausladen, A. & Fridovich, I. Superoxide and peroxynitrite inactivate aconitases, but nitric oxide does not. *J Biol Chem* **269**, 29405-8 (1994).
14. Rahman, S. et al. Leigh syndrome: clinical features and biochemical and DNA abnormalities. *Ann Neurol* **39**, 343-51 (1996).
15. Bergmeyer, H.U. *Methods in Enzymatic Analysis*, (1974).
16. Navet, R. et al. Proton leak induced by reactive oxygen species produced during in vitro anoxia/reoxygenation in rat skeletal muscle mitochondria. *J Bioenerg Biomembr* (2006).
17. Jarmuszkiewicz, W. et al. Redox state of endogenous coenzyme q modulates the inhibition of linoleic acid-induced uncoupling by guanosine triphosphate in isolated skeletal muscle mitochondria. *J Bioenerg Biomembr* **36**, 493-502 (2004).
18. Tabernero, A. et al. Activation of the peroxisome proliferator-activated receptor alpha protects against myocardial ischaemic injury and improves endothelial vasodilatation. *BMC Pharmacol* **2**, 10 (2002).
19. Schoonjans, K. et al. PPARalpha and PPARgamma activators direct a distinct tissue-specific transcriptional response via a PPRE in the lipoprotein lipase gene. *Embo J* **15**, 5336-48 (1996).

SUPPLEMENTARY TABLE 1

QUANTITATIVE REAL TIME RT-PCR PRIMERS AND PROBES

Gene ID	Forward Primer	Reverse Primer	Probe
Phd1	5'-GGTACGTGAGGCATGTTGACAAT-3'	5'-CTTAACATCCCAGTTCTGATTCAGGTA-3'	5'-FAM-CCCACGGCGATGGGCGCT-TAMRA-3'
Phd2	5'-AGTCCCATGAAGTGATCAAGTTCA-3'	5'-ATCCGCATGATCTGCATGG-3'	5'-FAM-TGCCCACGTCAGAGAGCAACATCAC-TAMRA-3'
Phd3	5'-CAGACCGCAGGAATCCACAT-3'	5'-TTCAGCATCGAAGTACCAGACAGT-3'	5'-FAM-AGCCCTCCTATGCCACCAGGTACGC-TAMRA-3'
Hif-1	5'-TGAGCTCACATCTTGATAAAGCTTCT-3'	5'-GGGCTTTCAGATAAAAACAGTCCAT-3'	5'-FAM-AGACCACCGGCATCCAGAAGTTTTCTCA-TAMRA-3'
Hif-2	5'-CAGCTTCCTTCGGACACATAAG-3'	5'-CTGGTCGGCCTCAGCTTC-3'	5'-FAM-TCCTGTCCTCAGTCTGCTCTGAAAATGAATC-TAMRA-3'
Ppar	5'-GCCAGTACTGCCGTTTTCACA-3'	5'-TTTCAGTTTTGCTTTTTCAGATCTTG-3'	5'-FAM-TTGCATTGTGTGACATCCCGACAGACA-TAMRA-3'
Ppar-	5'-AGAACCGCAACAAGTGTCAGTACT-3'	5'-GGATAGCGTTGTGCGACATG-3'	5'-FAM-CGCTTCCAGAAGTGCCTGGCACTC-TAMRA-3'
Pdk1	5'-CCCCGATTCAGGTTCACG-3'	5'-CCCGGTCACTCATCTTCACA-3'	5'-FAM-CACGCTGGGCGAGGAGGATCTG-TAMRA-3'
Pdk2	5'-CATCTTTGATGGCAGCACCA-3'	5'-GACACGCTGCAGTTGGGAT-3'	5'-FAM-CACCCCAAACACATTGGCAGCATC-TAMRA-3'
Pdk4	5'-TTACACGTACTCCACTGCTCCAA-3'	5'-ACCAAAACCAGCCAAAGGG-3'	5'-FAM-ACCTGTGATGGACAATTCCCGGAATG-TAMRA-3'
Hk4	5'-GCACACGTGGTGCTTTTGAG-3'	5'-GCCTTCGGTCCCCAGAGT-3'	5'-FAM-TCTCCACCTGCGACACAAAACGGG-TAMRA-3'
Pfkm	5'-GCCGGCTCAGTGAGACAAG-3'	5'-TGGCACCTTCAGCAACAATG-3'	5'-FAM-ACCCGTGGCTCTCGTCTCAACATCA-TAMRA-3'
Pgk	5'-CTGTGGTACTGAGAGCAGCAAGA-3'	5'-CAGGACCATTCCAAACAATCTG-3'	5'-FAM-TAGCTCGACCCACAGCCTCGGCATAT-TAMRA-3'
Pkm2	5'-ACATTGACTCTGCCCCCATC-3'	5'-GCAGGCCCAATGGTACAAAT-3'	5'-FAM-CGGCCCGCAACACTGGCAT-TAMRA-3'
Gapdh	5'-ACGTGCCGCCTGGAGA-3'	5'-CCCTCAGATGCCTGCTTCA-3'	5'-FAM-CACCTTCTTGATGTCATCATACTTGGCAGG-TAMRA-3'
-actin	5'-AGAGGGAAATCGTGCGTGAC-3'	5'-CAATAGTGATGACCTGGCCGT-3'	5'-FAM-CACTGCCGCATCCTCTTCCTCCC-TAMRA-3'

SHRNA OLIGONUCLEOTIDES

shPhd1^{KD} **(Sense)**	5'-CACCGCTGCATCACCTGTATCTATTTCTCTTGAAAATAGATACAGGTGATGCAGC-3'
shPhd1^{CTR} **(Sense)**	5'-CACCGCTTAACCCGTATTGCCTATTTCTCTTGAAAATAGGCAATACGGGTTAAGC-3'
shPpar^{KD} **(Sense)**	5'-CACCGGAAGCCGTTCTGTGACATCATCTCTTGAATGATGTCACAGAACGGCTTCC-3'
shPpar^{CTR} **(Sense)**	5'-CACCGCTCAGGGCTAAGGTCTATGATCTCTTGAATCATAGACCTTAGCCCTGAGC-3'

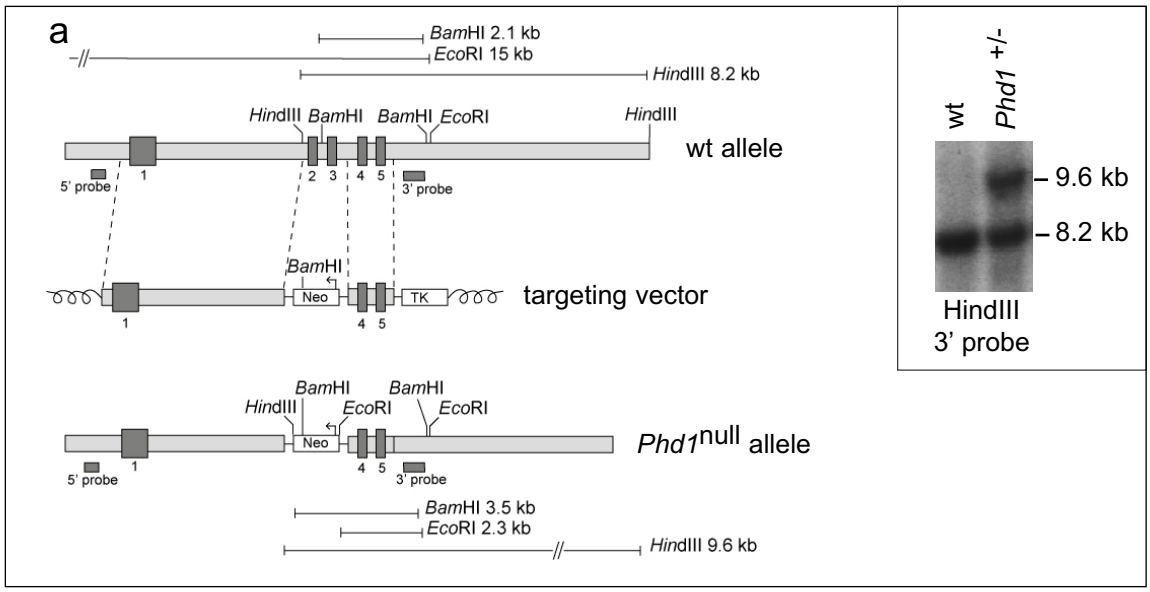

Supplementary Figure 1: *Generation of Phd1 deficient mice*

a, Targeting strategy for inactivation of the *Phd1* locus. Top: Wild-type *Phd1* allele, indicating the relative position of exons 1 to 5 (dark boxes in genomic structure). Middle: Outline of the targeting vector specifying the genomic sequences used as 5' and 3' homology flanks, cloned at both sides of a neomycine resistance (neo) cassette. A *thymidine kinase* (TK) gene outside the flanking homologies allowed for negative selection against random integration events. Bottom: Replacement of exon 2 and 3 by the neo cassette after homologous recombination. Diagnostic restriction fragments are indicated with their relative size by the thin lines under or above the alleles. ***Inset***, Southern blot analysis of genomic DNA from recombinant ES cells, digested with HindIII and hybridized with 3' external probe. The 8.2 kb and 9.6 kb genomic fragments correspond to wt and *Phd1*null alleles, respectively. Location of HindIII sites and probe are indicated in (***a***); wt, wild-type .